Tenth International Conference on Computational Fluid Dynamics (ICCFD10), Barcelona, Spain, July 9-13, 2018

ICCFD10-110

A new shock capturing approach based on the jump of conservation variables for discontinuous Galerkin methods

Zhao Hui*, Chen JiangTao* Liu Wei* and Li Bin*
Corresponding author: zbhui@mail.ustc.edu.cn

* China Aerodynamics Research and Development Center, China

Abstract: A new shock capturing approach based on the jump of conservation variables is proposed in this paper under the frame of artificial viscosity method, which has been widely accepted recently. The new method is designed for better adaptability and can be easily extended to non-uniform grid. The performance of the method is assessed by several typical cases. The result of isentropic vortex problem shows that the new approach is capable to produce the expected truncation error without polluting smooth flow. The simulations of one-dimensional shock tube problem show that spurious oscillations can be perfectly suppressed even with high order. For the simulation of flow over RAE2822 airfoil, the result is improved with the increase of the order of the scheme. As shown in the hypersonic cylinder flow case, the capability of the new method for shock capturing is demonstrated. Comparing with other artificial viscosity methods, this new method shows advantages over convergence and influence in smooth flow.

Keywords: discontinuous Galerkin, Artificial viscosity, Shock capturing, Hypersonic flow, Convergence.

1 Introduction

High order methods have received great focus and been applied to the simulations of turbulent flows and multi-scale problems[1-6] recently due to their favourable features in terms of accuracy, spectral properties, compactness, flexibility for unstructured mesh. They are still undergoing rapid developments in various aspects such as shock capturing, implicit time integration, grid adaptivity, and so on. For high order unstructured methods such as discontinuous Galerkin (DG), shock capturing with high order is still very challenging.

The current shock capturing methods are generally classified into three categories: limiter, reconstruction and artificial viscosity. For limiter method[7-10], the slope of solution on trouble element would be limited by some limiter functions and the corresponding accuracy would be spoiled. Unfortunately, the limiter method has some inherent disadvantages, such as the difficulty in marching the solution to a steady-state. Furthermore, since the limiting process is applied outside of the residual calculation, the solution that satisfies a zero steady-state residual has spurious oscillations in it.

Reconstruction methods such as WENO[11,12] and Hermite WENO(HWENO)[13] are alternative approaches to retain the higher-order modes and utilize the additional degrees of freedom to yield sharper shock transitions. Compared to WENO, HWENO-based methods are able to effectively achieve the compact stencil, and are thus more suitable for unstructured mesh. Another large family of shock capturing for unstructured high order methods is the artificial viscosity method[14-16,18,19], which explicitly add in this additional dissipation in the region of discontinuities by introducing viscous terms to the governing partial differential equation, and has achieved considerable success. The key for the artificial viscosity method is the right scaling, i.e. to decide the appropriate value of a shock sensor to activate the artificial viscosity. There has been plenty of work in this area.

A new shock capturing approach is proposed in this paper under the frame of artificial viscosity method. The performance of the method is assessed by several typical cases. The result of isentropic vortex problem shows that the new approach is capable to guarantee the accuracy of the solution under high order, and has little effect on the smooth region. The simulations of one-dimensional shock tube problem show that the correct position of the artificial viscosity is added and spurious oscillations can be perfectly suppressed in high-order conditions. For the simulation of flow over RAE2822 airfoil, the result is improved with the increase of the order of the scheme. Finally, as shown in the hypersonic cylinder flow case, the capability of the new method for shock capturing is demonstrated.

2 Numerical Methods

For conservation equation as follows:

$$\frac{\partial U}{\partial t}+\nabla\cdot F^{c}=0 \tag{1}$$

U represent the conservation variables of flow field, F^c represent the inviscid flux. The purpose of the artificial viscosity method is to increase the dissipation in the shock region so as to ensure a smooth transition in the shock region. In order to simplify the construction process, the Laplacian artificial viscosity model is chosen. Formula (1) is converted into the following form.

$$\frac{\partial U}{\partial t}+\nabla\cdot F^{c}-\nabla\cdot F^{s}=0 \tag{2}$$

F^s is artificial viscosity term, The specific form is as follows:

$$F^{s}=\nu_{s}\nabla U \tag{3}$$

ν_s represents the coefficient of artificial viscosity. Integrate equation (2) and ignore the boundary integral of the artificial viscosity term to obtain the following form:

$$\int_{\Omega}\phi\frac{\partial U}{\partial t}d\Omega+\oint_{\partial\Omega}\phi F^{c}\cdot\vec{n}-\int_{\Omega}\nabla\phi\cdot F^{c}d\Omega+\int_{\Omega}\nu_{s}(\nabla\phi\cdot\nabla U)=0 \tag{4}$$

Under normal circumstances, the distribution of the artificial viscous coefficient changes with the distribution of discontinuous regions such as shock waves. It is large enough near the shock wave, which can effectively suppress the oscillation, however in the smooth area in the flow field it is a small amount, which does not affect the accuracy of the smooth solution. The dimension of the artificial viscous coefficient is consistent with the kinematic viscosity coefficient and its performance is as follows:

$$\nu_{s}\sim VL \tag{5}$$

V represents the dimension of speed, L represents the dimension of length. the artificial viscosity coefficient, based on the dimension of VL, is constructed by using the constant variable jump at the interface of the grid cell and the pressure detector in the cell. For any cell, the jump of the boundary in a cell is defined as:

$$\nu_{jump}=\frac{[u_m]}{\overline{u_m}} \tag{6}$$

$[u_m]=\left|u_m^{+}-u_m^{-}\right|$ represents the jump of the conservation variables at the interface. $\overline{u_m}=\left|u_m^{+}+u_m^{-}\right|$ Represents the average of them. The conservation variables' jump of the boundary is assigned to the element in a normalized manner. The specific normalization method is as follows:

$$\nu_{\Omega}=\frac{\int_{\partial\Omega}\nu_{jump}ds}{Vol} \qquad (7)$$

Vol represents the volume of a cell. Using the pressure gradient in a cell, the pressure detector can be configured as follows.

$$f_p=\frac{|\nabla p|}{p+\delta} \qquad (8)$$

δ is a small amount that prevents the denominator from being zero.
Finally, the coefficient of artificial viscosity in a cell is constructed as follows:

$$\nu_s=C_{\varepsilon}\nu_{\Omega}f_p|V|h^2 \qquad (9)$$

In the above equation, V represents the speed within the cell, h represents the reference scale. C_{ε} is an empirical parameter and generally takes 0.1.

3 Numerical Results

3.1 The isentropic vortex problem

The isentropic vortex problem describes the addition of an isentropic vortex to the initial mean flow $\{\rho,\mathrm{u},\mathrm{v},\mathrm{p}\}=\{1,1,1,1\}$. The size of the vortex is given by:

$$\begin{cases}\delta u=-\dfrac{\varepsilon}{2\pi}e^{\frac{1-r^2}{2}}(\mathrm{y}+5)\\ \delta v=-\dfrac{\varepsilon}{2\pi}e^{\frac{1-r^2}{2}}(x+5)\\ \delta T=\dfrac{(\gamma-1)\varepsilon^2}{8\gamma\pi^2}e^{1-r^2}\\ \delta S=0\end{cases}$$

In the above formula, density, pressure and entropy are respectively expressed as $\rho,\mathrm{p},\mathrm{S}$. $r^2=(\mathrm{x}+5)^2+(\mathrm{y}+5)^2$, $\varepsilon=5.0$, The entire calculation area is $[-10,0]\times[-10,0]$, u , v respectively, represents the velocity component of the direction of x , y , the expression of entropy is $S=p/\rho^{\gamma}$, and the specific heat ratio $\gamma=1.4$. The isentropic vortex problem has an exact solution to verify the accuracy of the two-dimensional Euler problem.

In the calculation process, the boundary conditions are given according to the exact solution, and the time is advanced to 2s using the BDF2 scheme. We choose a hybrid grid for calculations. The reference grid and encryption grid are shown below.

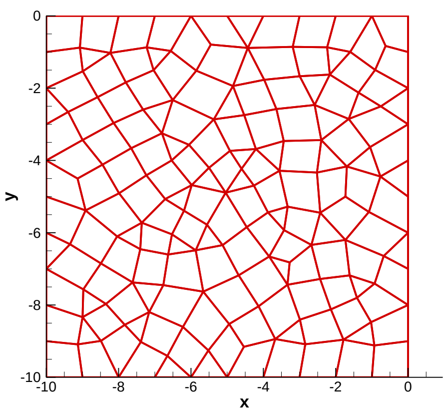

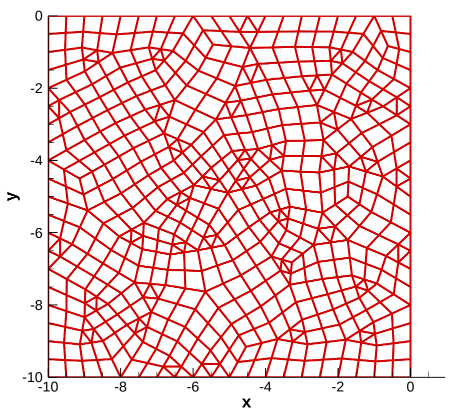

Base Grid(145) Refined Grid(145*4)

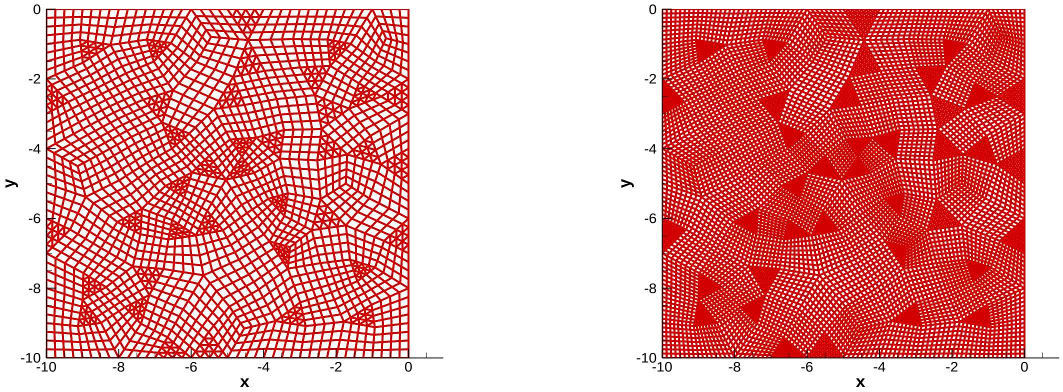

Refined Grid(145*16) Refined Grid(145*64)

Fig. 1 The uniform refined grid series for isentropic vortex problem

With or without artificial viscosity, entropy increase with grid scale and accuracy is shown in Figure 2. we can see that without adding artificial viscosity, the L1 norm and the L2 norm of the entropy increase from 2nd to 4th order can be consistent with the theoretical value, which can effectively guarantee the order. Once the artificial viscosity is added, the entire solving equation will change correspondingly. This is equivalent to adding a dissipative term in the flow field region, and the entire entropy increase in the flow field will inevitably become larger. Considering that the isentropic vortex flow is a smooth flow, the effect of the new artificial viscosity method on the smooth area should theoretically be a small amount. As can be seen from Figure 2, after adding artificial viscosity, the increase in entropy slightly increased, but the overall consistency with the absence of artificial viscosity, indicating that the artificial viscosity method has little effect on the smooth area.

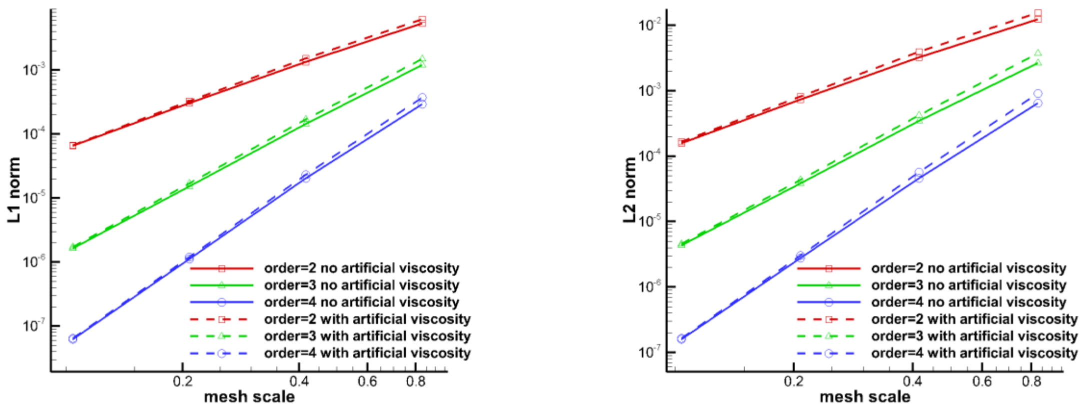

Fig. 2 Accuracy comparison for isentropic vortex problem (L1 norm(Left) L2 norm(Right))

3.2 One-dimensional Sod problem

$$(\rho, \mathrm{u}, \mathrm{p}) = \begin{cases} (1, 0, 1) & \mathrm{x} \le 0.5 \\ (0.125, 0, 0.1) & \mathrm{x} > 0.5 \end{cases}$$

The initial conditions of the one-dimensional Sod problem are given by the above formula, with initial breaks at $x = 0.5$. In the calculation area, a total of 100 units were subdivided and the end time of calculation is 0.2 s. Figure 3 shows a comparison of the density distributions calculated at different order, where exact is the theoretical solution. As can be seen, this method can also suppress non-physical oscillations better than the limiter method while maintaining high resolution. From the distribution of artificial viscosity in Fig. 4, the artificial viscosity mainly distributes in the shock region, and there is almost no increment in the smooth region. With the improvement of the precision, the distribution of the artificial viscosity becomes more reasonable.

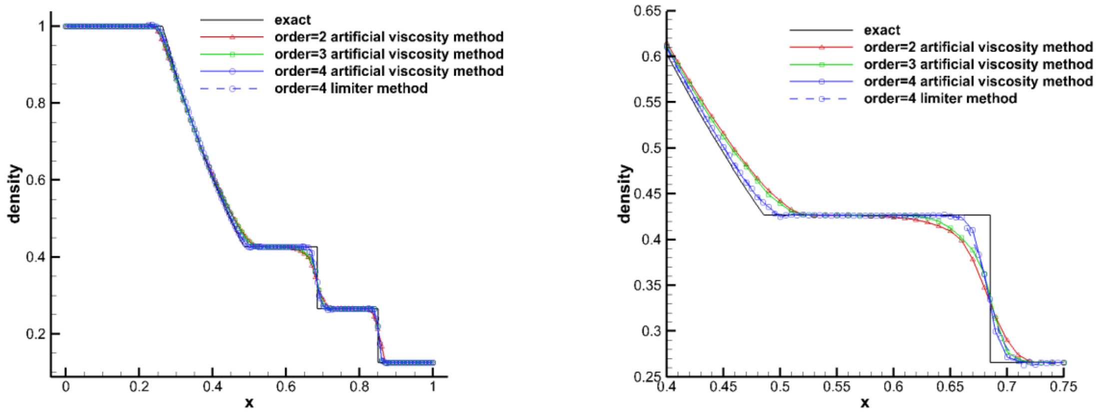

Fig. 3 Density distribution

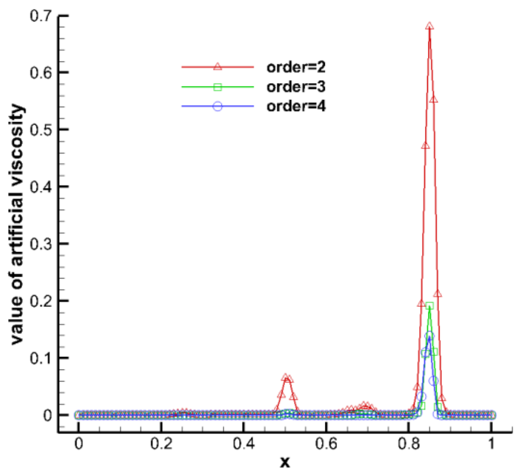

Fig. 4 Value of artificial viscosity distribution

3.3 Calculation of Airfoil Flow in RAE2822

In order to investigate the performance of the proposed method on transonic flow field shock capture, Hartmann's method was chosen for comparison. The calculations for the RAE2822 airfoil were performed and the calculation state was set as $Ma_\infty = 0.729$ the attack angle $\alpha_\infty = 2.31°$. The corresponding calculation grid is shown in Figure 5 below. The amount of cells is 10,000. the obtained airfoil surface pressure distribution is shown in Figure 6. It can be seen from the figure that as the order increases, it becomes more and more “sharp”, and is closer and closer to the results in reference [17]. Under the second-order accuracy, the pressure distribution curve obtained by this method is closer to the reference value, especially in the shock region, the pressure curve The performance is more "sharp", but under the fourth-order accuracy, the pressure distribution curves obtained by the two methods are not much different. Figure 8 shows the distribution of artificial viscosity in the flow field calculated by the two methods under different accuracy. As the order increases, the artificial viscosity is more and more concentrated in the shock region and the airfoil leading edge. Combined with the convergence of Figure 9, under the condition of transonic speed, this method can better suppress non-physical oscillations compared to Hartmann method. The method we developed can effectively avoid the influence on the smooth region of the flow field under the condition of ensuring convergence.

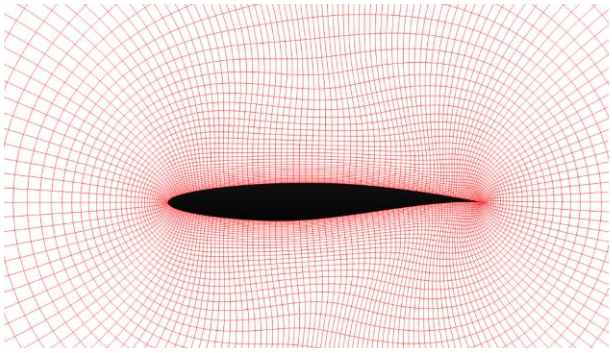

Fig. 5 Mesh of RAE2822

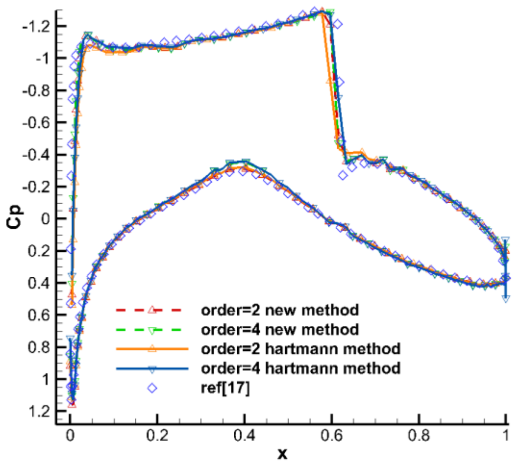

Fig. 6 Cp distribution

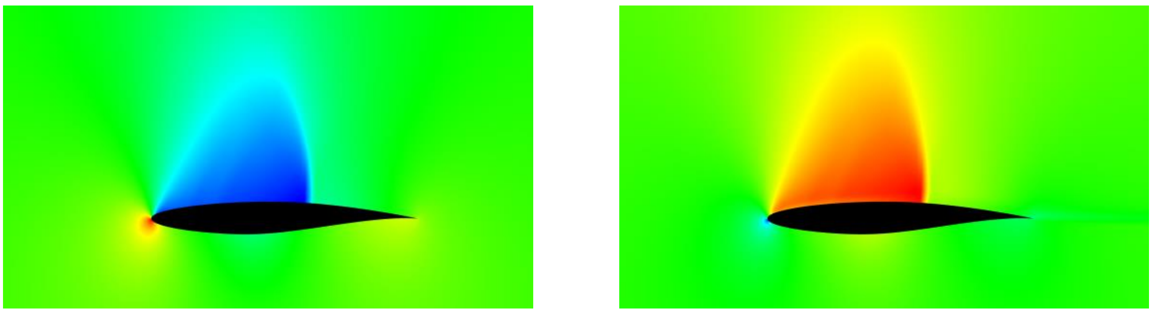

Fig. 7 Contour of pressure（Left） and Mach number（Right）

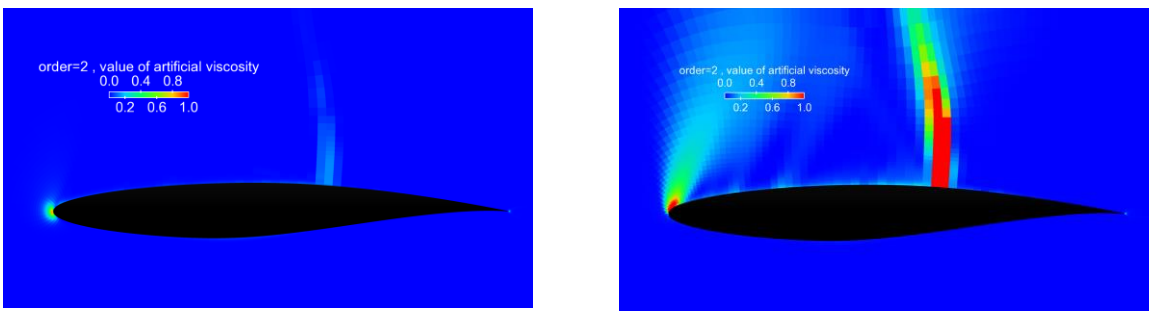

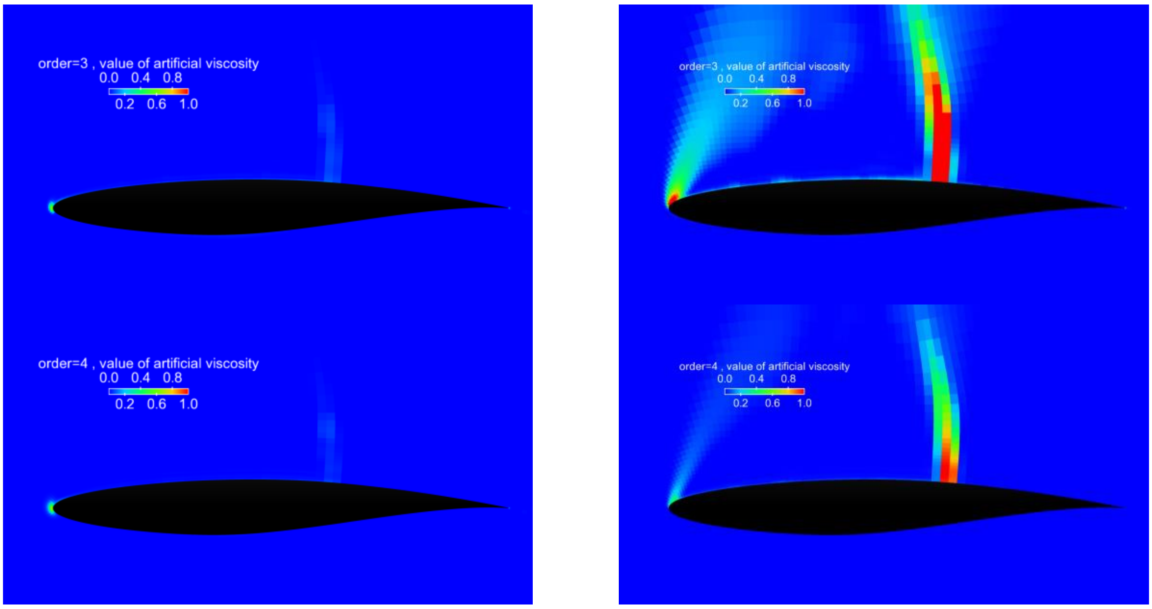

Fig. 8 Distribution of value of artificial viscosity

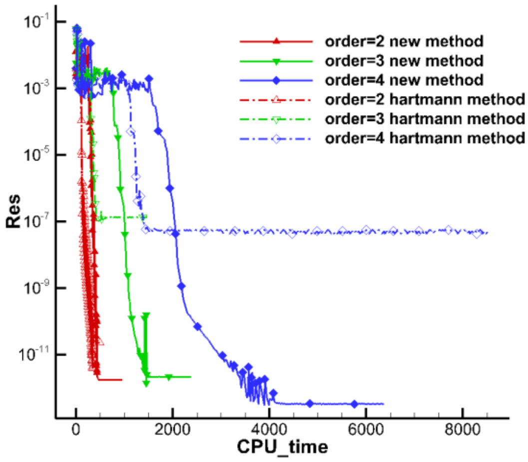

Fig. 9 Comparison of residual history

3.4 Hypersonic Half Cylindrical Problem

In order to investigate the adaptability of the artificial viscosity method in the hypersonic state, a hypersonic half-cylindrical case was selected for testing. The number of free flow Mach number is 4 and the calculation accuracy is 5th order. The calculation grid is shown in Figure 10. The total number of mesh cells is 640, and the number of mesh cells which are close to a semi-cylindrical surface is 32. The minimum distance from the first mesh of the near wall surface to the wall surface is half the cylinder diameter. In the case of 5th-order accuracy, the contours of the density, Mach number, and the distribution of artificial viscosities are shown in Figures 11 and 12. It can be clearly seen that the contours of density and Mach number are smooth and clear, the distribution is consistent, the shock waves are effectively captured, and the artificial viscosity is mainly concentrated in the shock wave area. By comparing the distribution of artificial viscosity, it can be clearly found that the artificial viscosity distribution obtained by our new method has a narrower range than the Hartmann's method. The "pollution" of the smooth area is relatively small. Combined with the convergence of the two methods in Figure 13, the new method's performance is better under hypersonic conditions, which is basically consistent with the Hartmann's method.

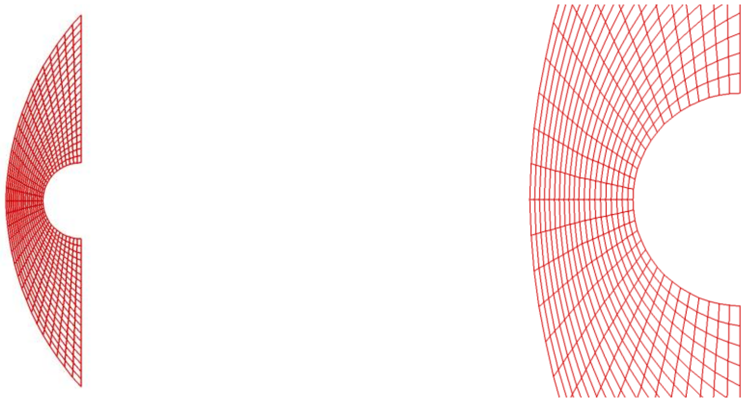

Fig. 10 Computational mesh for the supersonic cylinder flow

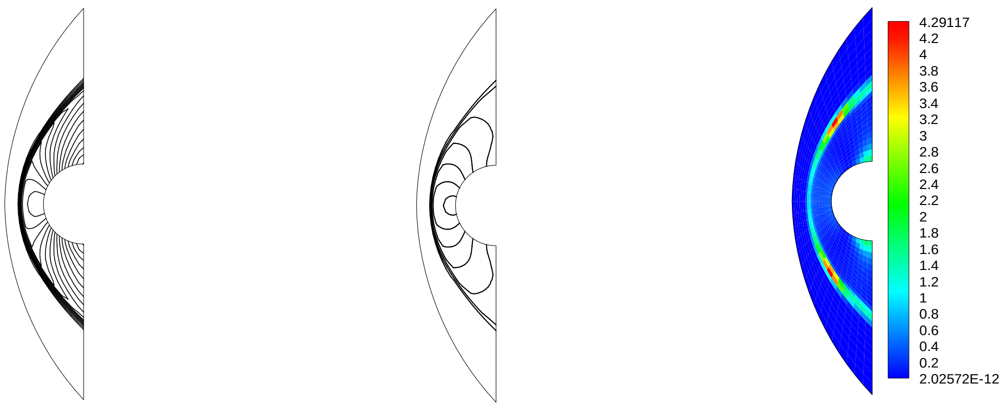

Density Mach Artificial viscosity

Fig. 11 The contours of density, Mach number and artificial viscosity(new method)

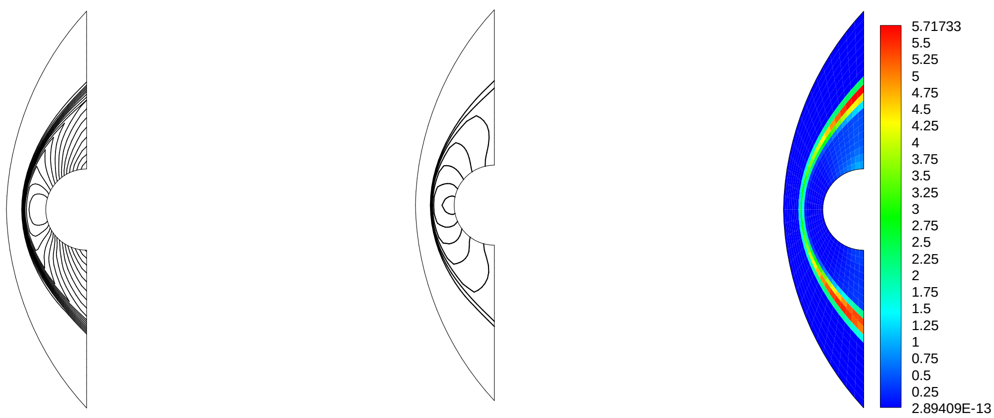

Density Mach Artificial viscosity

Fig. 12 The contours of density, Mach number and artificial viscosity (Hartmann method)

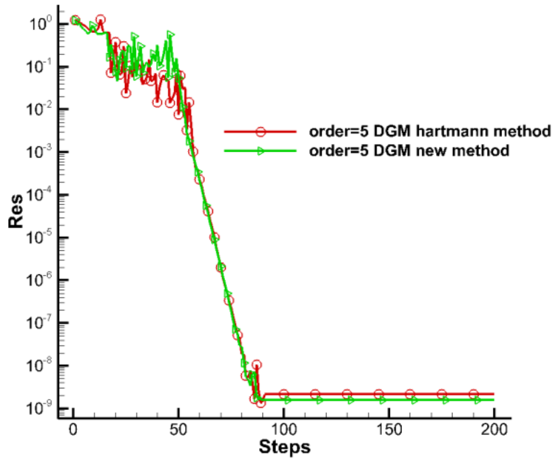

Fig. 13 comparison of residual history

4 Conclusion and Future Work

We propose a step-based high-accuracy DG artificially viscous shock wave capture method. A series of test examples are used to evaluate the method. The comparison of isentropic vortex cases with and without artificial viscosity can be found in this paper. The artificial viscosity method has very little "pollution" in the smooth area and almost no loss in overall accuracy. The one-dimensional Sod example shows that the method can also suppress non-physical oscillations and trap shock waves effectively compared to the limiter method. With the increase of the order, the performance of artificial viscosity is also significantly improved. In the two-dimensional case, RAE2822 transonic velocity and semi-cylindrical hypersonic examples show that compared with Hartmann's artificial viscous shock wave capture method, this method has less influence on the smooth region under the same calculation results. Compared with the Hartmann's method, the new approach has certain advantages in convergence.

The artificially viscous shock wave capturing method proposed in this paper has a simple formula that contains only one free parameter and is easy to program. This method can effectively guarantee the convergence while effectively suppressing the oscillation, and has less pollution to the flow field in the smooth region. In the case of high order, the proposed method has certain advantages over the Hartmann's method in terms of convergence.

References

[1] Tam C K W. Computational aeroacoustics: Issues and method [J]. AIAA Journal, 1995. 1788–1796.

[2] Tam C K W. Advances in numerical boundary conditions for computational aeroacoustics. Journal of Computational Acoust, 1998. 377-402.

[3] Tam C K W. Computational aeroacoustics, A Wave Number Approach. London: Cambridge University Press, 2012.

[4] Smagorinsky J. General circulation experiments with the primitive equations I. the basic experiment. Monthly Weather Rev, 1963. 99-105

[5] Lesieur M, Metais O. New trends in large eddy simulations of turbulence. Annu Rev Fluid Mech, 1996. 45–82.

[6] Sagaut P. Large eddy simulation for incompressible flows, an introduction. 3rd ed. Heidelberg:

Springer-Verlag; 2006.
[7] Harten, A., Engquist, B., Osher, S. & Chakravarthy, S. R. Uniformly high order accurate essentially non-oscillatory schemes, III. J. Comput. Phys. 1987. 231–303
[8] Barth T J, Jespersen D. The design and application of upwind schemes on unstructured meshes. Proceedings of the 27th AIAA Aerospace Sciences Meeting, Reno, NV, AIAA Paper. 1989. 89-0366
[9] Venkatakrishnan V. Convergence to steady state solutions of the Euler equations on unstructured grids with limiters. J. Comput. Phys. 1995. 120-130
[10]Park J S, Yoon S H, Kim C. Multi-dimensional limiting process for hyperbolic conservation laws on unstructured grids. J. Comput. Phys., 2010. 788-812.
[11]Shi, J., Hu, C. & Shu, C. A Technique of Treating Negative Weights in WENO Schemes. J. Comput. Phys. 2000. 108–127
[12]Qiu, J. & Shu, C.-W. Hermite WENO schemes and their application as limiters for Runge–Kutta discontinuous Galerkin method: one-dimensional case. J. Comput. Phys. 2004. 115–135
[13]Luo, H., Baum, J. D. & Löhner, R. A Hermite WENO-based limiter for discontinuous Galerkin method on unstructured grids. J. Comput. Phys.2007. 686–713
[14]Hartmann, R. Adaptive discontinuous Galerkin methods with shock-capturing for the compressible Navier-Stokes Equations. Int. J. Numer. Meth. Fluids, 2006.1131–1156
[15]Hartmann, R. and Houston, P. Adaptive Discontinuous Galerkin Finite Element Methods for the Compressible Euler Equations. J. Comput. Phys., 2002. 508–532
[16]Aliabadi, S., Tu, S.-Z., and Watts, M. An alternative to limiter in discontinuous Galerkin finite element method for simulation of compressible flows. AIAA Paper 2004-76
[17]Guo Yong-heng, Research of Discontinuous Galerkin Method for Hyperbolic Conservation Equations[PhD Thesis].Xi'an: Northwestern Polytechnical University,2013
[18]Persson, P.-O. & Peraire, J. Sub-cell shock capturing for discontinuous Galerkin methods. AIAA Pap. 2006. 112
[19]Barter, G. E. & Darmofal, D. L. Shock capturing with PDE-based artificial viscosity for DGFEM: Part I. Formulation. J. Comput. Phys. 2010. 1810–1827